Two-dimensional polymer photonic crystal band-edge lasers fabricated by nanoimprint lithography

V. Reboud, P. Lovera, and N. KehagiasM. ZelsmannC. Schuster, F. Reuther, and G. GruetznerG. RedmondC. M. Sotomayor Torres

Citation: Appl. Phys. Lett. **91**, 151101 (2007); doi: 10.1063/1.2798250
View online: http://dx.doi.org/10.1063/1.2798250
View Table of Contents: http://aip.scitation.org/toc/apl/91/15
Published by the American Institute of Physics

Two-dimensional polymer photonic crystal band-edge lasers fabricated by nanoimprint lithography

V. Reboud,[a] P. Lovera, and N. Kehagias
Tyndall National Institute, Lee Maltings, Prospect Row, Cork, Ireland

M. Zelsmann
LTM-CNRS, c/o CEA-LETI, 17 rue des martyrs, F-38054 Grenoble Cedex 9, France

C. Schuster, F. Reuther, and G. Gruetzner
Micro Resist Technology GmbH, Koepenicker Str. 325, Haus 211, 1255 Berlin, Germany

G. Redmond
Tyndall National Institute, Lee Maltings, Prospect Row, Cork, Ireland

C. M. Sotomayor Torres
Tyndall National Institute, Lee Maltings, Prospect Row, Cork, Ireland; Catalan Institute of Nanotechnology, Campus de Bellaterra, Edifici CM7, 08193 Bellaterra, Barcelona, Spain; and Catalan Institute for Research and Advanced Studies ICREA, 08010 Barcelona, Spain

(Received 17 August 2007; accepted 23 September 2007; published online 8 October 2007)

We report on the fabrication and characterization of two-dimensional polymer photonic crystal band-edge lasers operating in the visible range. The components have been fabricated in a dye chromophore-loaded polymer matrix by nanoimprint lithography. High-symmetry band-edge modes are used to generate laser emission. The experimental lasing frequencies are in good agreement with those calculated using a two-dimensional plane wave algorithm. These results demonstrate the potential of nanoimprint lithography for the fabrication of two-dimensional planar photonic crystal structures in an active medium in a one-step process. © *2007 American Institute of Physics*.
[DOI: 10.1063/1.2798250]

The advantages of two-dimensional (2D) defect-free photonic crystals (PhCs) over the conventional one-dimensional (1D) feedback gratings are to present potentially lower lasing thresholds[1] and highly directional vertical emission.[2] The 2D optical feedback is provided by the low-group velocity band-edge modes of the 2D PhC.[3,4] In the past few years, PhC band-edge lasers have attracted great interest and have been demonstrated in organic[4–7] and semiconductor[8–11] media. Recently, this research field has been highlighted by the demonstration of an electrically driven PhC laser.[12] Despite such progress, the fabrication of PhCs often requires elaborate and expensive techniques, such as electron-beam lithography and reactive ion etching.[13] For this reason, PhC lasers are not yet extensively used. Cost and time efficient lithographic techniques are actually desirable to solve this throughput issue. In this context, several patterning methods have been developed. For example, laser holography demonstrated its capability to pattern perfectly the periodic 2D (Refs. 7 and 14) and three-dimensional[15] PhCs on a large scale. Soft lithography[16] and nanoimprint lithography[17] (NIL) techniques have been used to realize 1D feedback grating with high throughput. NIL has been used to fabricate 2D photonic crystals for enhanced light extraction.[18,19] Moreover, room temperature NIL has been proposed to minimize the degradation of the active media due to the otherwise higher temperatures.[20,21] Unfortunately, the former promising method does not lead to high aspect ratio features. Therefore, due to the relatively weak optical feedback, the dimension of the gratings has to be increased to obtain lasing action. In this letter, we report on 2D visible PhC band-edge lasers fabricated in a single processing step by NIL. The active medium is the printable polymer itself loaded with dye emitting molecules. The devices were designed to operate at the Γ band-edge points above the cone of light. We demonstrate that NIL can achieve a high fidelity and high aspect ratio pattern transfer. This results in larger feedback of the lasing modes and thus reduces laser thresholds and device sizes.

Silicon stamps for two-dimensional photonic crystals with honeycomb lattices were produced by electron beam lithography (Jeol 6000) with a dose of 130 $\mu C/cm^2$ and under a beam current of 100 pA using a 150 nm thick layer of ZEP 520 resist (Zeon Corporation) prebaked at 120 °C. The development is carried out during 30 s in a solution of ZED N50 (Zeon Corporation). The silicon stamp is etched 350 nm deep using an inductively coupled plasma reactive ion etching system (Surface Technology System) with a mixture of SF_6 and C_4F_8 gases. The overall stamp size used in our experiments is a 2×2 cm^2 silicon stamp, including 100×100 μm^2 PhC areas. The stamp is subsequently treated with an antiadhesive monolayer (tridecafluor-1, 1, 2, 2-tetrahydrooctyl trichlorosilane) deposited from the vapor phase, which results in a very low surface energy (between 10 and 11 mN/m). This treatment is very important in order to avoid adhesion of the polymer to the stamp during the imprinting process and to facilitate demolding. The dye-doped polymer is composed of rhodamine 6G (Sigma Aldrich) directly dissolved with a concentration of 5×10^{-3} mol/l in a printable polymer (mr-NIL 6000 from Micro Resist Technology), which has a glass transition temperature of only 40 °C and is optically transparent in the visible range. The refractive index of the doped polymer has been

[a]Electronic mail: vincent.reboud@tyndall.ie

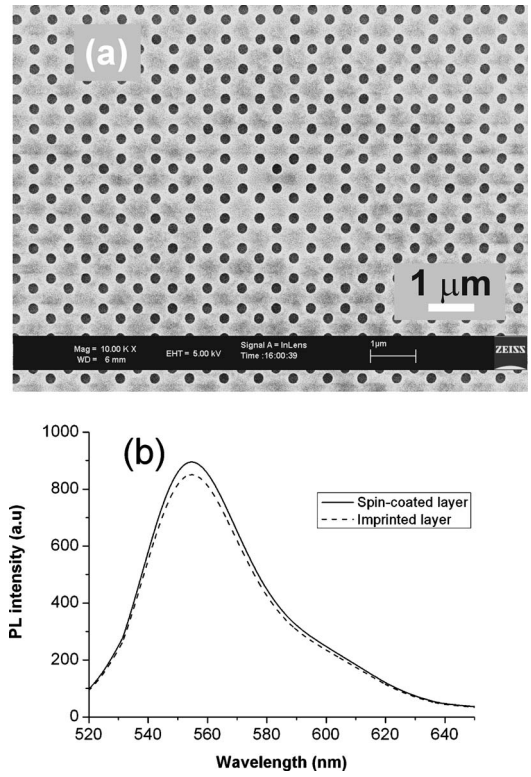

FIG. 1. (Color online) (a) Scanning electron microscopy (SEM) micrograph of nanoimprinted photonic crystal in mr-NIL 6000 containing rhodamine 6G with a lattice constant of 460 nm. (b) Emission spectra of rhodamine 6G in mr-NIL 6000 taken before (solid line) and after (dot line) the nanoimprint process.

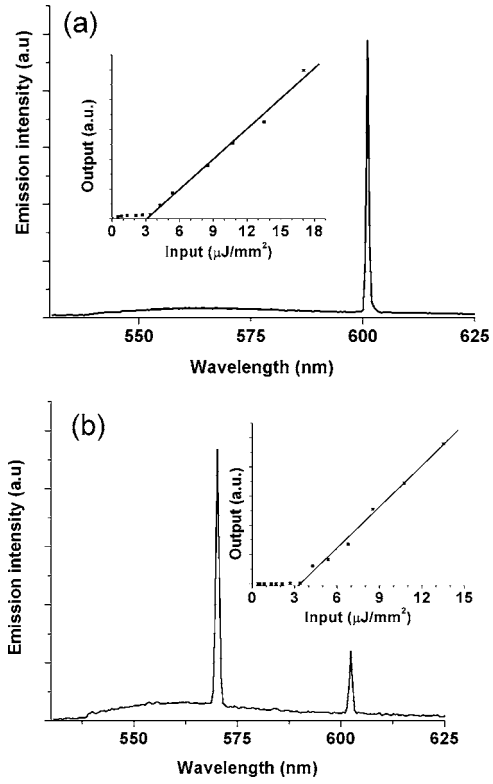

FIG. 2. (Color online) (a) PL spectrum of the 2D PhC with the 460 nm lattice constant under a pulsed excitation of 17 $\mu J/mm^2$. (b) PL spectrum of the 2D PhC with the 580 nm lattice constant under a pulsed excitation of 13.5 $\mu J/mm^2$. Insets: Peak emission intensity vs absorbed excitation fluence associated to each PhC.

measured by ellipsometry to a value of 1.614 at a wavelength of 550 nm.

During the nanoimprint lithography process, the stamp is pressed directly into a thin resist film at a temperature above the glass transition temperature of the polymer under high pressure in a 2.5 in. Obducat nanoimprinting machine. The modified mr-NIL 6000 resist is spin coated on a Pyrex substrate at 3000 rpm for 1 min and baked at 115 °C for 5 min to remove the residual solvent. The measured polymer thickness is 280 nm. Then, the stamp is pressed against the substrate at a temperature of 90 °C and under a pressure of 60 bars for 5 min. The pressure is sustained until the temperature falls below 35 °C. Imprints were not exposed to UV light to crosslink the polymer. Figure 1(a) shows the scanning electron microscopy images of nanoimprinted photonic crystals with a lattice constant of 460 nm.

To test the possible impact of the NIL process on the optical properties of the active layer, the photoluminescence (PL) spectrum of the spin-coated dye-doped polymer on a quartz substrate was compared to that of the same substrate imprinted with a flat stamp. For this measurement, PL was excited by the 514.5 nm line of an argon ion laser, collected through a 20× microscope objective and dispersed in a spectrometer with 0.1 nm spectral resolution. A decrease of less than 3% in the PL intensity is found after patterning [Fig. 1(b)]. This effect is due to the temperature sensitivity of rhodamine 6G during the prebaking and imprinting process, while the imprinting pressure is not found to be a critical parameter.[22] The use of a printable polymer with a glass transition temperature of about 40 °C, which is much lower than that of, e.g., polymethyl methacrylate, is therefore an advantage to avoid thermal degradation.

The 2D nanoimprinted PhCs were also characterized by PL spectroscopy at room temperature in a vacuum cell. In this case, the samples were optically pumped using a 10 Hz frequency-doubled Q-switched $Nd:VO_4$ laser light at 532 nm focused to a 40 μm diameter spot on the sample surface. The temporal width of the pulses emitted by the laser is 0.7 ns. Figure 2(a) shows the measured emission spectrum of the 2D PhC with a 460 nm lattice constant at a pump power of 17 $\mu J/mm^2$, i.e., 5.6 times above the laser threshold. The measurable linewidth of the laser peak is limited by the resolution of the spectrometer. The emission intensity is plotted as a function of the incident excitation fluence. The light input-output relation exhibits a sharp turn on at the laser threshold. By changing the lattice constant of the PhC, one can explore other lasing modes from the PhC. For example, by fixing the lattice constant to 580 nm, one can observe two other modes in the gain bandwidth of rhodamine [Fig. 2(b)].

To explain these observations and to compare the measured lasing wavelengths to simulation, the 2D band diagram of the 2D PhC with a honeycomb lattice was calculated using a plane wave algorithm from Optiwave Corporation. Figure 3 presents the dispersion diagram for the photons propagating in the plane of the PhC around the Γ point for the transverse electric (TE) and the transverse magnetic (TM) polarizations.

A minimum lasing threshold of 3 $\mu J/mm^2$ was obtained for the PhC with the lattice constant of 460 nm. This lasing threshold is 2.5 times lower and the laser surface is 50 times

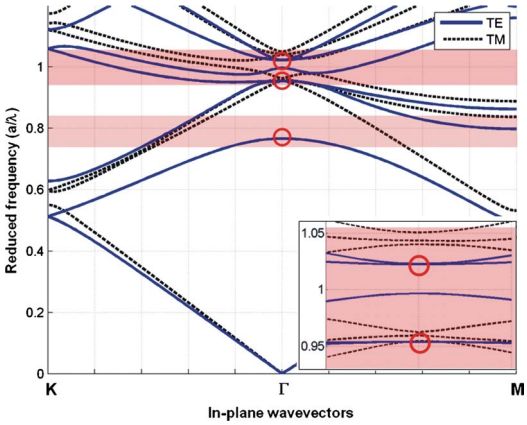

FIG. 3. (Color online) Photonic band structure of a honeycomb lattice of air hole PhC calculated with a plane wave–basis frequency-domain method (dotted lines: TM polarization; solid lines: TE polarization), where a is the lattice constant and λ is the wavelength. Hole radius is $R=0.24a$. Lower and upper red bands correspond to the gain bandwidth of rhodamine 6G (550–610 nm in wavelength) for PhC lattice constants $a=460$ nm and $a=580$ nm, respectively. Inset: Band diagram zoom from the reduced frequency from 0.92 to 1.06.

smaller than those measured for the 1D nanoimprinted organic feedback grating, made of Rhodamine 6G doped SU-8 polymer.[23] The laser with the 460 nm lattice constant operates at 601 nm, 51 nm above the maximum of the spontaneous emission peak, indicating a strong optical feedback provided by the PhC at the Γ band-edge points above the light cone. At these points, the photonic bands are flat and the group velocity approaches zero. By comparing the experimental results with the flat bands of the calculated band diagram, we can observe that the lasing modes are associated with the TE polarization (circles in Fig. 3). Furthermore, this is in agreement with the fact that TE modes are expected to present lower losses than TM modes because TE modes have a higher effective refractive index and, therefore, a higher confinement than TM modes. Table I shows a comparison of the calculated and measured reduced frequencies of the lasing modes. A very good agreement between numerical and experimental values is found.

The lifetime of the lasers as function of the number of excitation pump pulse at 8.5 $\mu J/mm^2$ (corresponds to 2.8 times the laser threshold) was also measured. The laser emission drops exponentially to 10% of its initial values after 8200 pulses, which is comparable to solid-state dye lasers emitting in the visible wavelengths.[24] To improve the lifetime of the lasers, a solution is to replace the dye molecules with semiconductor nanocrystals with optical gain[25] embedded in a printable polymer.[20]

In summary, two-dimensional polymer photonic crystal band-edge lasers fabricated by nanoimprint lithography have been realized. Nanoimprint lithography offers a large scale patterning method at high resolution and high throughput. Optically driven lasing response of the honeycomb lattice surface-emitting photonic band-edge lasers is identified at the Γ band-edge point of the defect-free PhCs by the measurement of the spectral position. This behavior agrees very well with the theoretical calculation by a plane wave method. These results could be applied for the fabrication of cost-efficient light-emitting polymer devices in optoelectronics.

TABLE I. Comparison of the calculated and measured reduced frequencies for the PhC band-edge lasers with the lattice constants $a=460$ nm [one lasing mode, Fig. 1(a)] and $a=580$ nm [two lasing modes, Fig. 2(b)].

Lattice constant (nm)	460	580	
Calculated reduced frequency (a/λ)	0.766	0.954	1.022
Measured reduced frequency (a/λ)	0.765	0.962	1.017

The support of the EC-funded project NaPa (Contract No. NMP4-CT-2003-500120), of the EC-funded project PHOREMOST (FP6/2003/IST/2-511616), and of the Science Foundation Ireland (Grant No. 02/IN.1/172) is gratefully acknowledged. The content of this work is the sole responsibility of the authors.

[1] C. Bauer, H. Giessen, M. Schanel, E. B. Kley, C. Schmitt, U. Scherf, and R. F. Mahrt, Adv. Mater. (Weinheim, Ger.) **13**, 1161 (2001).
[2] A. Mekis, A. Dodabalapur, R. Slusher, and J. D. Joannopoulous, Opt. Lett. **25**, 942 (2000).
[3] M. Imada, S. Noda, A. Chutinan, T. Tokuda, M. Murata, and G. Sasaki, Appl. Phys. Lett. **75**, 316 (1999).
[4] M. Meier, A. Mekis, A. Dodabalapur, A. Timko, R. E. Slusher, J. D. Joannopoulous, and O. Nalamasu, Appl. Phys. Lett. **74**, 7 (1999).
[5] N. Moll, R. F. Mahrt, C. Bauer, H. Giessen, B. Schnabel, E. B. Kley, and U. Scherf, Appl. Phys. Lett. **80**, 734 (2000).
[6] M. Notomi, H. Suzuki, and T. Tamamura, Appl. Phys. Lett. **78**, 1325 (2001).
[7] R. Harbers, J. Hoffnagle, W. Hinsberg, R. F. Mahrt, N. Moll, D. Erni, and W. Bachtold, Appl. Phys. Lett. **87**, 241124 (2005).
[8] C. O. Cho, J. Jeong, J. Lee, I. Kim, D. H. Jang, Y. S. Park, and J. C. Woo, Appl. Phys. Lett. **87**, 161102 (2005).
[9] S. H. Kwon, H. Y. Ryu, G. H. Kim, Y. H. Lee, and S. B. Kim, Appl. Phys. Lett. **83**, 3870 (2003).
[10] C. Monat, C. Seassal, X. Letartre, P. Regreny, P. Rojo-Romeo, P. Viktorovitch, M. Le Vassord Yerville, D. Cassagne, J. P. Albert, E. Jalaguier, S. Pocas, and B. Aspar, Appl. Phys. Lett. **81**, 5102 (2002).
[11] H. Y. Ryu, S. H. Kwon, Y. J. Lee, and J. S. Kim, Appl. Phys. Lett. **80**, 3476 (2002).
[12] H. G. Park, S. H. Kim, S. H. Kwon, Y. G. Ju, J. K. Yang, J. H. Baek, S. B. Kim, and Y. H. Lee, Science **305**, 1444 (2004).
[13] S. Noda, A. Chutinan, and M. Imada, Nature (London) **407**, 608 (2000).
[14] C. O. Chi, J. Jeong, J. Lee, H. Jeon, I. Kim, D. H. Jang, Y. S. Park, and J. C. Woo, Appl. Phys. Lett. **87**, 161102 (2005).
[15] X. Wang, J. F. Xu, H. M. Su, Z. H. Zeng, H. Z. Wang, Y. K. Pang, and W. Y. Tam, Appl. Phys. Lett. **82**, 2212 (2003).
[16] A. Roger, M. Meier, A. Dodabalapur, E. J. Laskowski, and M. A. Capuzzo, Appl. Phys. Lett. **74**, 3257 (1999).
[17] D. Pisignano, L. Persano, P. Visconti, R. Cingolani, G. Gigli, G. Barbarella, and L. Favaretto, Appl. Phys. Lett. **83**, 2545 (2003).
[18] V. Reboud, N. Kehagias, M. Zelsmann, M. Striccoli, M. L. Curri, A. Agostiano, M. Tamborra, M. Fink, F. Reuther, G. Gruetzner, and C. M. Sotomayor Torres, Appl. Phys. Lett. **90**, 011115 (2007).
[19] V. Reboud, N. Kehagias, M. Zelsmann, C. Schuster, M. Fink, F. Reuther, G. Gruetzner, and C. M. Sotomayor Torres, Opt. Express **15**, 7190 (2007).
[20] E. Mele, A. Camposeo, R. Stabile, P. Del Carro, F. Di Benedetto, L. Persano, R. Cingolani, and D. Pisignano, Appl. Phys. Lett. **89**, 131109 (2006).
[21] P. Del Carro, A. Camposeo, R. Stabile, E. Mele, L. Persano, R. Cingolani, and D. Pisignano, Appl. Phys. Lett. **89**, 201105 (2006).
[22] F.-H. Ko, L.-Y. Weng, C.-J. Ko, and T.-C. Chu, Microelectron. Eng. **83**, 864 (2006).
[23] M. B. Christiansen, M. Schøler, and A. Kristensen, Opt. Express **15**, 3931 (2007).
[24] A. Costela, I. Garcia-Moreno, J. M. Figuera, F. Arnat-Guerri, R. Mallavia, M. D. Santa-Maria, and R. Sastre, J. Appl. Phys. **80**, 3167 (1996).
[25] V. I. Klimov, S. A. Ivanov, J. Nanda, M. Achermann, I. Bezel, J. A. McGuire, and A. Piryatinski, Nature (London) **447**, 441 (2007).